Permanent Single-Line-to-Ground Fault Removal Method for Ferro-Resonance Avoidance in Neutral Ungrounded Distribution Network

PAN LU[1], WEN WANG[1], (Member, IEEE), QIAN YU[2], BISHUANG FAN[1], (Member, IEEE), PENGFEI LIU[3], FALIANG WANG[4], AND XIANGJUN ZENG[1], (Senior Member, IEEE)

[1]College of Electrical and Information Engineering, Changsha University of Science and Technology, Changsha 410114, China
[2]College of Business Administration, Hunan University of Finance and Economics, Changsha 410205, China
[3]State Grid Hunan Electric Power Company, Yongzhou 410029, China
[4]State Grid Jiangxi Electric Power Company, Yichun 336000, China

Corresponding author: Qian Yu (yuqian@hufe.edu.cn)

ABSTRACT In the neutral ungrounded distribution network, the removal of permanent single-line-to-ground (SLG) fault easily leads to saturation of the electromagnetic voltage transformers (PT), which may cause ferroresonance overvoltage and PT failure. This paper analyzes the zero-sequence voltage after the removal of the SLG fault and reveals the mechanism of ferroresonance excited by the removal of the SLG fault. Then, the total power and transient energy of the zero-sequence circuit under the SLG fault are analyzed. It is deduced that the energy reaches the minimum value at the zero-cross point (ZCP) of the neutral voltage. Based on this, a permanent SLG fault removal method to avoid ferroresonance is proposed, which uses the ZCP point as the fault removal instant. Simulations in ATP-EMTP show that the proposed method can effectively avoid ferroresonance on subharmonic mode. It can also enhance the ferroresonance suppression performance of the ferroresonance suppression resistor in the fundamental-frequency and high-frequency conditions.

INDEX TERMS Distribution network, permanent single-line-to-ground fault, ferroresonance avoidance, fault removal instant.

I. INTRODUCTION

Ferroresonance often occurs between the electromagnetic voltage transformer (PT) and distributed phase-to-ground capacitances in neutral ungrounded distribution network as power system disturbances happen [1]. The overvoltage caused by the ferroresonance not only endangers the insulation of power supply equipment, but also generates continuous over-current which burns out the power supply apparatus, resulting in serious power failure.

Many factors could excite ferroresonance, such as three-phase breakers asynchronously switch-on [2], removal of the single-line-to-ground (SLG) fault [3] or sharply load change [4]. Under these conditions, the zero-sequence voltage increases and may result in saturation of PT excitation

The associate editor coordinating the review of this manuscript and approving it for publication was Ali Raza[ID].

inductance. The saturated inductance is smaller than the inductance in normal (unsaturated) state, which forms a parameter matching the phase-to-ground capacitances at typical frequencies. In the ferroresonance excitation factors, the removal of SLG fault happens frequently [5]–[7]. During the SLG fault, the sound phase voltages increase, and large amount of energy is stored in the phase-to-ground storage elements. When the SLG fault is removed, the energy can only be released through the zero-sequence circuit path which is slightly damped. If the energy is large enough, the current of PT excitation inductance will be larger than the linear current threshold, resulting in saturation and consequently ferroresonance [8]–[10].

Various modes of ferroresonance are identified based on the associated waveforms and classified into fundamental, subharmonic, quasi-periodic, and chaotic modes [11], [12]. The type of ferroresonance is closely related to the
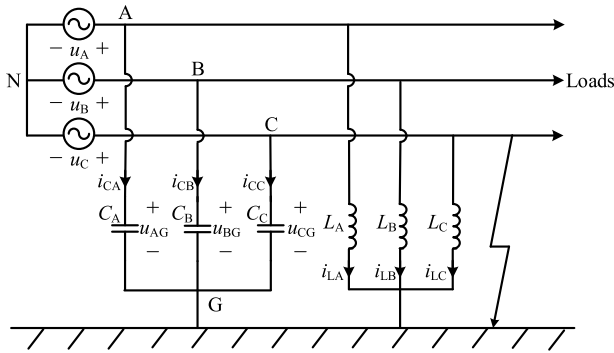
FIGURE 1. Simplified circuit of the ungrounded distribution network when the SLG fault happens.

phase-to-ground capacitance. With the increase of the phase-to-ground capacitance, the frequency of ferroresonance decreases [13], [14].

The passive and active methods are presented to suppress the ferroresonance. The passive methods include broadening the linear range of PT excitation inductance, adopting 4PT method and increasing the system capacitance to the ground [15]. To prevent the occurrence of ferromagnetic resonance, the system parameters can be kept away from the resonance condition by changing the system parameters. The active methods include connecting linear or nonlinear resistors in open delta winding of PT, grounding the neutral point of the primary side of PT through large resistance, grounding the neutral point of the system through resistance, etc., which can effectively suppress ferroresonance [16], [17].

In these literatures, the ferroresonance suppression measures have been widely investigated, however, the avoidance of ferroresonance after the SLG fault has not been researched. This paper firstly analyzes the ferroresonance mechanism of the neutral ungrounded network after the SLG fault. The theoretical analysis shows that the occurrence of ferroresonance is closely related to the system energy represented by the initial values of inductance current and capacitance voltage at the time of fault removal. It is then revealed that the system energy reaches the minimum value when the zero-sequence voltage is zero. This paper then proposes a permanent SLG fault removal method to avoid ferroresonance and the implementation flowchart is presented. Simulation results show that the proposed method can effectively avoid ferroresonance in subharmonic mode, and enhance the performance of the ferroresonance suppression resistor in fundamental-frequency and high-frequency conditions.

II. MECHANISM OF FERRORESONANCE EXCITED BY THE REMOVAL OF SLG FAULT

To analyze the ferroresonance brought about by the removal of the SLG fault, a simplified circuit diagram of an ungrounded distribution network is established as shown in Fig. 1. The distributed phase-to-ground capacitances are C_X (X = A, B, or C). It is assumed the three-phase capacitances are balanced, i.e., $C_X = C$. Compared with the PT excitation

inductance, the line impedance and PT leakage inductance are smaller, which can be ignored. To create the worst-case scenario, the damping factors are all ignored, i.e., the distributed leakage resistance of the feeder line and the PT leakage resistance can be both ignored. Therefore, the electromagnetic PT is simplified to the excitation inductance. The there-phase inductances are assumed to be balanced when in the unsaturated state, i.e., $L_X = L$. A bolted and permanent SLG fault is set to occur at phase C.

During the SLG fault, the phase-to-ground voltage of phase C u_{CG} becomes zero. Those of phase A and phase B (u_{AG} and u_{BG}) increase to line-to-line voltages. Current standards require that the inflection voltage of the PT is larger than the line voltage ($>1.9U_m/\sqrt{3}$ in China, where U_m is the nominal line voltage). It means the phase voltage of the PT does not exceed the inflection voltage during the SLG fault and thus the excitation inductance can be considered linear. In a very short time after the fault is removed, the PT inductance voltage gradually approaches the inflection voltage, and the excitation inductance changes from the linear region to the saturation region. Thus, the states of the PT after the removal of the faulty line can be divided into two stages, i.e., the unsaturated stage and the saturated one, following the timed sequence. Thus, the excitation inductances of the sound phases are unsaturated during the fault. After the fault is removed by disconnecting the fault feeder breaker, the energy of the storage elements in the sound phases transfers between the phase-to-ground capacitances and the excitation inductances. This may push the inductances into the saturated region and cause ferroresonance. The inductance voltages can be used as an indicator of ferroresonance. If the voltages exceed the PT inflection voltage threshold, the inductance enters the saturated region and ferroresonance happens. Therefore, in the first stage, i.e., between the SLG fault removal and the ferroresonance occurrence, the excitation inductances are still in the unsaturated region and the circuit is thus linear and the analysis methods for linear system can be used. The following analysis mainly focuses on the linear stage.

A. LINEAR STAGE ANALYSIS AFTER SLG FAULT REMOVAL
From the circuit theory, the circuit in the linear stage can be divided into two kinds of circuits, i.e., the zero-state response circuit and the zero-input response circuit. In the zero-state response circuit, the initial voltages of the phase-to-ground capacitances u_{XG10} and the initial currents of PT excitation inductances i_{LX10} are all zero and the three-phase parameters are balanced as shown in Fig. 2. As both the power supply and storage elements are balanced, the neutral voltage in the zero-state response circuit is zero, i.e., $u_{NG1} = 0$.

The zero-input response circuit is shown in Fig. 3. The initial capacitance voltages and inductance currents in the sound phases, u_{XG20} and i_{LX20}, which depend on the fault removal instant, are no longer zero. At the instant of fault removal, the capacitance voltage and inductance current on the fault phase are zero, i.e., $u_{CG20} = 0$ and $i_{LC20} = 0$. The
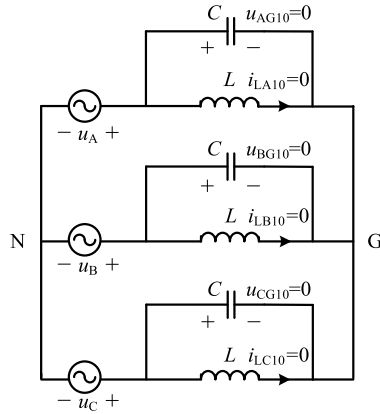
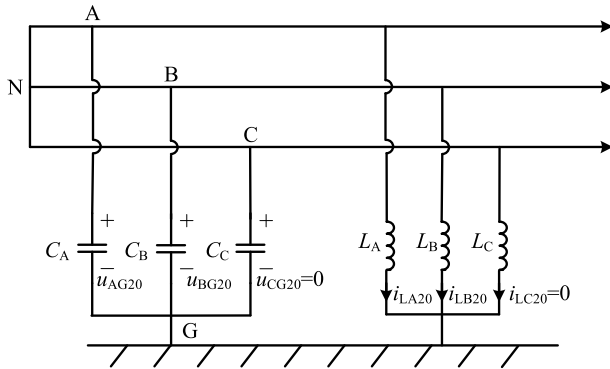**FIGURE 2.** Zero-state response circuit after the removal of SLG fault.

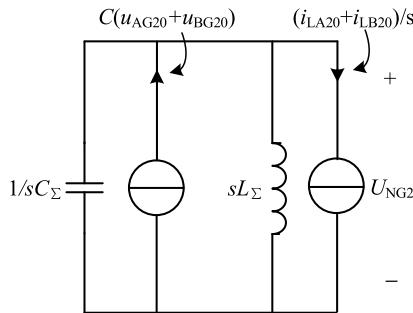**FIGURE 3.** Zero-input response circuit after the removal of SLG fault.

FIGURE 4. Laplace transformation of zero-input circuit.

zero-input response circuit can be simplified to Fig. 4 by the Laplace transform, where $C_\Sigma = 3C$ and $L_\Sigma = L/3$. From Fig. 4, the neutral voltage equation can be obtained as

$$(3sC + \frac{3}{sL})U_{NG2} = C(u_{AG20} + u_{BG20}) - \frac{i_{LA20} + i_{LB20}}{s} \tag{1}$$

Based on the inverse Laplace transformation, the zero-input neutral voltage in the time domain can be expressed as

$$u_{NG2} = \frac{1}{3}\sqrt{(u_{AG20} + u_{BG20})^2 + \omega_r^2 L^2 (i_{LA20} + i_{LB20})^2} \sin \\ \times (\omega_r t - \varphi + \pi), \tag{2}$$

where $\omega_r = 1/(LC)^{1/2}$ and $\varphi = \arctan \frac{u_{AG20} + u_{BG20}}{9\omega_r L(i_{LA20} + i_{LB20})}$.

Therefore, from the superposition theorem, in the linear period after the SLG fault removal, the neutral voltage equals
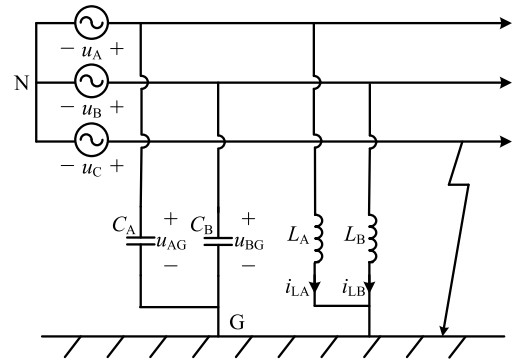

FIGURE 5. The simplified SLG fault circuit for initial value calculation.

to the sum of its values in the zero-state response and the zero-input response, i.e., $u_{NG} = u_{NG1} + u_{NG2} = u_{NG2}$.

B. INITIAL VALUE CALCULATION FROM THE SLG FAULT CIRCUIT

The initial values of the capacitance voltages and inductance currents can be obtained by the SLG fault circuit, shown in Fig. 5. The phase angle of u_A is set to be zero and the amplitude of nominal phase voltage is denoted by U_m. The phase-to-ground voltages of the sound phases at the fault removal instant $(t = t_0)$ can be expressed as

$$\begin{cases} u_{AG0} = \sqrt{3}U_m \sin(\omega_n t_0 - \frac{\pi}{6}) \\ u_{BG0} = \sqrt{3}U_m \sin(\omega_n t_0 - \frac{\pi}{2}), \end{cases} \tag{3}$$

where ω_n is the fundamental angular frequency. Assume that the fault circuit has reached the steady state, then the sum of the excitation inductor currents of the sound phases at the fault removal instant can be obtained from (3).

$$i_{LA0} + i_{LB0} = \frac{3U_m}{\omega_n L}\sin(\omega_n t_0 - \frac{5\pi}{6}) = i_{LA20} + i_{LB20} \tag{4}$$

The sum of the capacitance voltages of the sound phases can also be obtained from (3).

$$u_{AG0} + u_{BG0} = 3U_m \sin(\omega_n t_0 - \frac{\pi}{3}) = u_{AG20} + u_{BG20} \tag{5}$$

Combined (2), (4) and (5), the amplitude of the neutral voltage u_{NG} in (2) can be expressed as

$$\begin{aligned} ||u_{NG2}|| &= \frac{U_m}{\sqrt{2}}\sqrt{k + 1 + (k - 1)\cos(2\omega_n t_0 - \frac{2\pi}{3})} \\ &= ||u_{NG}||, \end{aligned} \tag{6}$$

where k is the ratio of the phase-to-ground capacitive reactance to the PT inductive reactance, i.e., $k = \frac{1}{\omega_n^2 LC}$.

C. CONSISTENCY TO THE EXPERIMENTAL CONCLUSION

Fig. 6 is the 3D diagram of standardized voltage $||u_{NG}||^*$ by the nominal phase voltage amplitude concerning the fault removal instant t_0 and the ratio k, i.e., $||u_{NG}||^* = ||u_{NG}||/U_m$. It can be seen that when k is fixed,
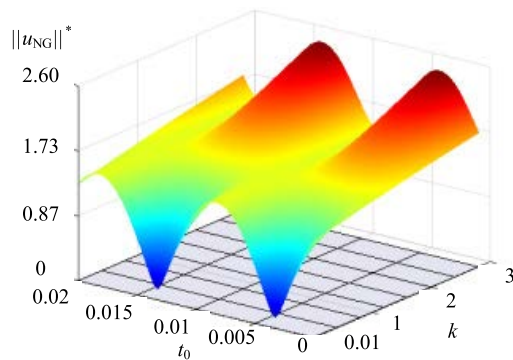
FIGURE 6. Diagrams of $\|u_{NG}\|^*$ with the change of t_0 and k.
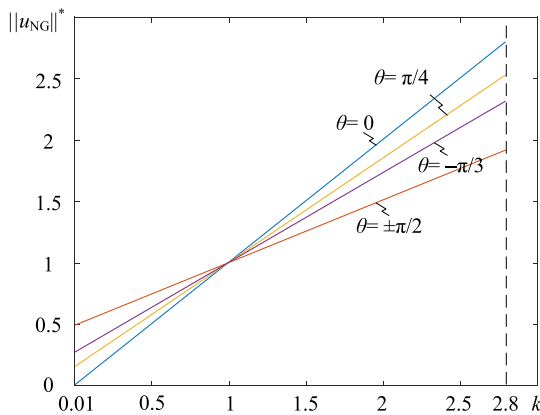

FIGURE 7. Diagrams of $\|u_{NG}\|^*$ with the change of k and θ.

$\|u_{NG}\|^*$ changes periodically with t_0. When t_0 is fixed, $\|u_{NG}\|^*$ monotonously increases with the increase of k.

The phase angle of the neutral voltage at the fault removal point is denoted by θ, which equals $2\omega_n t_0 - 2\pi/3$. Fig. 7 shows the waveform of $\|u_{NG}\|^*$ changing with k when θ is 0, $-\pi/4$, $-\pi/3$ and $\pm\pi/2$, respectively. It can be seen that when θ is fixed, with the increase of k, the neutral voltage amplitude $\|u_{NG}\|^*$ also increases. It is consistent with the experimental characteristics of ferroresonance that as k increases, the resonance frequency ω_n gets higher and the amplitude of the neutral voltage u_{NG} also gets higher, and thus ferroresonance is easier to be excited [18]. Fig. 7 also shows that the fault removal phase angle affects the amplitude of zero-sequence voltage. When the resonance frequency is low, i.e., k is large, the amplitude of u_{NG} reaches its minimum as $\theta = \pm\pi/2$. Nevertheless, when the resonance frequency is high, i.e., k is small, the amplitude of u_{NG} reaches its minimum as $\theta = 0$.

As the excitation inductance voltage is the sum of phase-to-neutral voltage and the zero-sequence voltage, proper selection of the fault removal phase angle can help reduce the excitation inductor voltage, and thus avoid ferroresonance.

III. FAULT REMOVAL INSTANT TO AVOID FERRORESONANCE

The fault removal instant to avoid zero-sequence overvoltage and ferroresonance can be derived from analysis of the circuit in Fig. 1. The initial phase angle of the u_A is set to zero.

According to the relationship of the three-phase voltages, we get

$$\begin{cases} u_A = U_m \sin \omega_n t \\ u_B = U_m \sin(\omega_n t - \dfrac{2\pi}{3}) \\ u_C = U_m \sin(\omega_n t + \dfrac{2\pi}{3}) \end{cases} \tag{7}$$

During the SLG fault, the line-to-ground voltages of phase A and B, u_{AG}, u_{BG}, can be expressed as

$$\begin{cases} u_{AG} = \sqrt{3}U_m \sin(\omega_n t - \dfrac{\pi}{6}) \\ u_{BG} = \sqrt{3}U_m \sin(\omega_n t - \dfrac{\pi}{2}) \end{cases} \tag{8}$$

It is assumed that the PT excitation inductances on the sound phases are not saturated at the SLG fault instant. i_{LAf} and i_{LBf} denote the PT excitation inductance currents on phase A and B at the SLG fault instant, respectively. The excitation inductance currents during the fault can be expressed as

$$\begin{cases} i_{LA} = -\dfrac{\sqrt{3}U_m}{\omega_n L} \cos(\omega_n t - \dfrac{\pi}{6}) + i_{LAf} \\ i_{LB} = -\dfrac{\sqrt{3}U_m}{\omega_n L} \cos(\omega_n t - \dfrac{\pi}{2}) + i_{LBf} \end{cases} \tag{9}$$

It can be seen from (9) that the inductance currents contain dc component related to the initial currents at the SLG fault instant.

During the SLG fault, the capacitance currents on the sound phases can be expressed as

$$\begin{cases} i_{CA} = C\dfrac{du_{AG}}{dt} = \sqrt{3}\omega_n CU_m \cos(\omega_n t - \dfrac{\pi}{6}) \\ i_{CB} = C\dfrac{du_{BG}}{dt} = \sqrt{3}\omega_n CU_m \cos(\omega_n t - \dfrac{\pi}{2}) \end{cases} \tag{10}$$

As the 10 kV windings of the power supply transformer and the load transformer are both in delta connection, there is no zero-sequence path from the primary side of the power supply to the secondary side of the load. The energy in the distributed line-to-ground capacitances and the PT excitation inductances of the sound phases exchanges between themselves. The instantaneous power p and total energy w of these storage elements can be expressed as

$$\begin{cases} p_A = u_{AG}(i_{LA} + i_{CA}) \\ p_B = u_{BG}(i_{LB} + i_{CB}) \\ w = \int_0^t (p_A + p_B)dt + w(0) \end{cases} \tag{11}$$

From (8) to (11), it can be obtained that

$$p_A = \sqrt{3}U_m \sin(\omega_n t - \frac{\pi}{6})[\sqrt{3}U_m(\omega_n C \\ - \frac{1}{\omega_n L})\cos(\omega_n t - \frac{\pi}{6}) + i_{LAf}] \tag{12}$$

$$p_B = \sqrt{3}U_m \sin(\omega_n t - \frac{\pi}{2})[\sqrt{3}U_m(\omega_n C \\ - \frac{1}{\omega_n L})\cos(\omega_n t - \frac{\pi}{2}) + i_{LBf}] \tag{13}$$

The total power p_Σ of the energy storage elements can be expressed as

$$p_\Sigma = p_A + p_B = \frac{3}{2}U_m^2(\omega_n C - \frac{1}{\omega_n L})\sin(2\omega_n t - \frac{2\pi}{3})$$
$$+ \sqrt{3}U_m i_{LAf}\sin(\omega_n t - \frac{\pi}{6})$$
$$+ \sqrt{3}U_m i_{LBf}\sin(\omega_n t - \frac{\pi}{2}) \qquad (14)$$

The energy w of the energy storage elements can be expressed as

$$w = \frac{1}{2}(Cu_{AG}^2 + Cu_{BG}^2 + Li_{LA}^2 + Li_{LB}^2) \qquad (15)$$

Combining (8), (9) and (15), we get

$$w = \frac{3U_m^2}{4}(C - \frac{1}{\omega_n^2 L})\cos(2\omega_n t + \frac{\pi}{3}) + \frac{3U_m^2}{2}(C + \frac{1}{\omega_n^2 L})$$
$$- \frac{\sqrt{3}U_m}{\omega_n}[i_{LAf}\cos(\omega_n t - \frac{\pi}{6}) + i_{LBf}\cos(\omega_n t - \frac{\pi}{2})]$$
$$+ \frac{L}{2}(i_{LAf}^2 + i_{LBf}^2) \qquad (16)$$

The first term in (16) is a double frequency component, corresponding to the steady state ac component of the total energy. The second term is constant, corresponding to its steady-state dc component. The rest term relates to the initial value of the excitation inductance currents, corresponding to the transient part of the total energy. The transient part of the total energy will decrease to zero if we consider the loss of the equivalent resistances of the zero-sequence circuit. Therefore, when the SLG fault occurs, after a brief transition process, the total energy of the system will be double frequency periodic with dc bias. Therefore, the minimum point of the system energy can be found, which can be used to avoid ferroresonance.

According to the transient process analysis above, the dc component of the excitation inductance currents generated by the fault disturbance decreases to zero after some time. Then, the system reaches the steady state, and the following expressions exist

$$\begin{cases} i_{LA} = -\frac{\sqrt{3}U_m}{\omega_n L}\cos(\omega_n t - \frac{\pi}{6}) \\ i_{LB} = -\frac{\sqrt{3}U_m}{\omega_n L}\cos(\omega_n t - \frac{\pi}{2}) \end{cases} \qquad (17)$$

The expression of the total power of the system in steady state can be obtained from (8), (10) and (17),

$$p_\Sigma = \frac{3}{2}U_m^2(\omega_n C - \frac{1}{\omega_n L})\sin(2\omega_n t - \frac{2\pi}{3}) \qquad (18)$$

From the relationship between the power and energy, when the total power of the system changes from negative to positive, the total energy of the storage elements reaches the minimum value. The time instant corresponding to the minimum can be expressed as

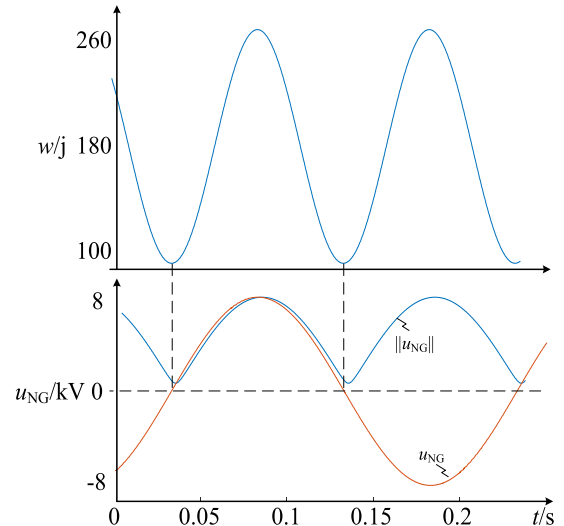$$t_{w\min} = \frac{(1+3n)\pi}{3\omega_n}, \qquad (19)$$

FIGURE 8. Comparison diagram of system energy and removal time.

where n is a natural number. The neutral voltage during the fault can be expressed as

$$u_{NG} = U_m \sin(\omega_n t - \frac{\pi}{3}) \qquad (20)$$

Combined (19) and (20), the neutral voltage at the time of $t_{w\min}$ can be obtained

$$u_{NG}(t_{w\min}) = 0 \qquad (21)$$

It can be seen from (21) that the total energy of the system reaches the minimum value when the neutral voltage crosses zero. Fig. 8 is a typical simulation waveform showing the relationship between the neutral voltage and the total energy after the SLG fault. It can be seen clearly that the zero-cross point of the neutral voltage corresponds to the minimum of the total energy and the neutral voltage amplitude.

For the storage elements, the excitation inductance and the phase-to-ground capacitance, their energies correspond to their state variables, voltage for capacitance and current for inductance. Therefore, great energy means large initial value of the state variable, which means the inductance voltage reaches the inflection point of its excitation characteristics quickly. Then, the ferroresonance is easy to happen. That is to say, the total energy of the system is an important factor to excite ferroresonance. Removing the fault at the minimum energy instant ensures that the least energy exchange between the storage elements avoids overvoltage and overcurrent in the excitation inductances. Therefore, removing the SLG fault at the zero-cross point of the neutral voltage can effectively avoid ferroresonance or help suppress ferroresonance.

IV. IMPLEMENTATION
According to the relationship between the neutral voltage and the total energy of the system, this paper proposes a processing method for the permanent SLG fault for neutral ungrounded distribution network. It reduces the probability
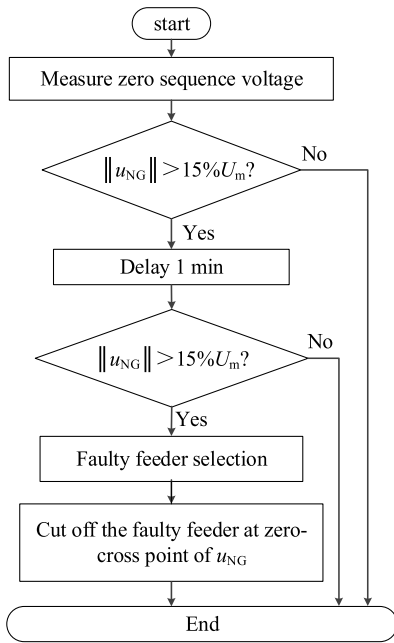
FIGURE 9. Flowchart permanent SLG fault removal.

FIGURE 10. Topology of the simulation model.

FIGURE 11. Exciting characteristic curve of PT.

TABLE 1. JDZJ-10 PT technical parameters.

Type	Nominal Voltage Ratio	Secondary Load /VA
JDZJ-10	10/√3：0.1/√3：0.1/3	40

TABLE 2. Excitation characteristic parameters of JDZJ-10 PT.

Group	1	2	3	4	5
I/mA	1.64	3.14	16.11	64.67	191.28
Ψ/Wb	14.51	25.71	41.42	59.63	66.36

of ferroresonance by cutting off the fault line at zero-cross point of the neutral voltage. The flowchart of permanent SLG fault removal is shown in Fig. 9.

Firstly, the neutral voltage and the three-phase voltages are measured. Secondly, the comparison between the neutral voltage and the voltage threshold of 15% of the rated phase voltage is used to determine whether the SLG fault happens [19], [20]. Then, according to the requirements of distribution network technical guidelines, 1 min delay is set to avoid the transient of the SLG fault, and it is assured after the delay the system enters the steady state. If the amplitude of u_{NG} is still higher than the SLG fault voltage threshold, the permanent SLG fault will be judged to happen. Then, the selection of the fault feeder is carried out to determine which feeder is at fault. Finally, zero-cross point of the neutral voltage is detected, and the fault feeder is cut off at the detected zero-cross point.

A practical issue is about how to ensure the right phase angle of the faulty line disconnecting as the opening time of the circuit breaker is not fixed. The proposed method for ferroresonance avoidance can be implemented with the assistance of the circuit breaker with short arcing time, e.g., the fast vacuum circuit breaker (FVCB). The typical arcing time of the FVCB is less than 5 ms [21]. As the inherent opening time is fixed and the opening time of the FVCB is the addition of the inherent opening time and the arcing time, the FVCB can be used to cut off the faulty line at the instant around the zero-cross point of the neutral voltage.

V. SIMULATION VERIFICATION
The simulation model of the 10 kV neutral ungrounded distribution network is built in ATP-EMTP. The single-phase topology of the model is shown in Fig. 10. There are three
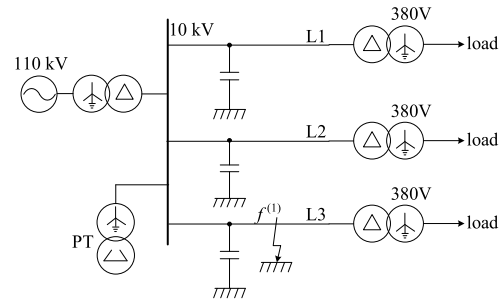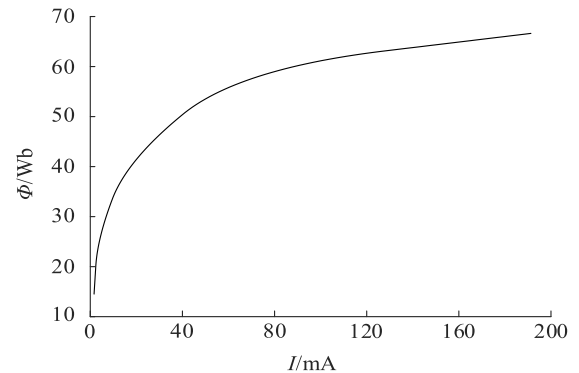
10 kV feeder lines from the busbar and the length of each feeder is assumed to be equal. The fundamental frequency of the system is 50 Hz. The capacitance-to-ground per kilometer is 0.05 μF/km. Each load resistance is 0.5 ohm per phase, and it corresponds to a total power of 290 kW. The PT model is JDZJ-10, its technical parameters are shown in Tab. 1 and its excitation characteristics are shown in Tab. 2 and Fig. 11.

In the simulation, the SLG fault is set at 0 s with a ground-fault resistance of 0.1 Ω. The fault is removed at the zero-cross point of neutral voltage (hereinafter referred to as ZCP) or the maximum point of neutral voltage (hereinafter referred to as MP). In the present research, the type of ferroresonance can be judged according to the frequency spectrum of neutral voltage when ferroresonance occurs [22].

A. SUB-HARMONIC RESONANCE CONDITION
Assume that the total length of the feeder lines is 60 km, and the capacitance-to-ground is 3 μF. Fig. 12a to Fig. 12c show

(a) Line-to-ground voltages while cutting off the fault feeder at the MP.

(b) Neutral voltage waveform while cutting off the fault feeder at the MP.

(c) Spectrum of the neutral voltage after cutting off the fault feeder at the MP

(d) Line-to-ground voltages while cutting off the fault feeder at the ZCP.

(e) Line-to-ground voltages while cutting off the fault feeder at the ZCP when the Line is unbalanced.
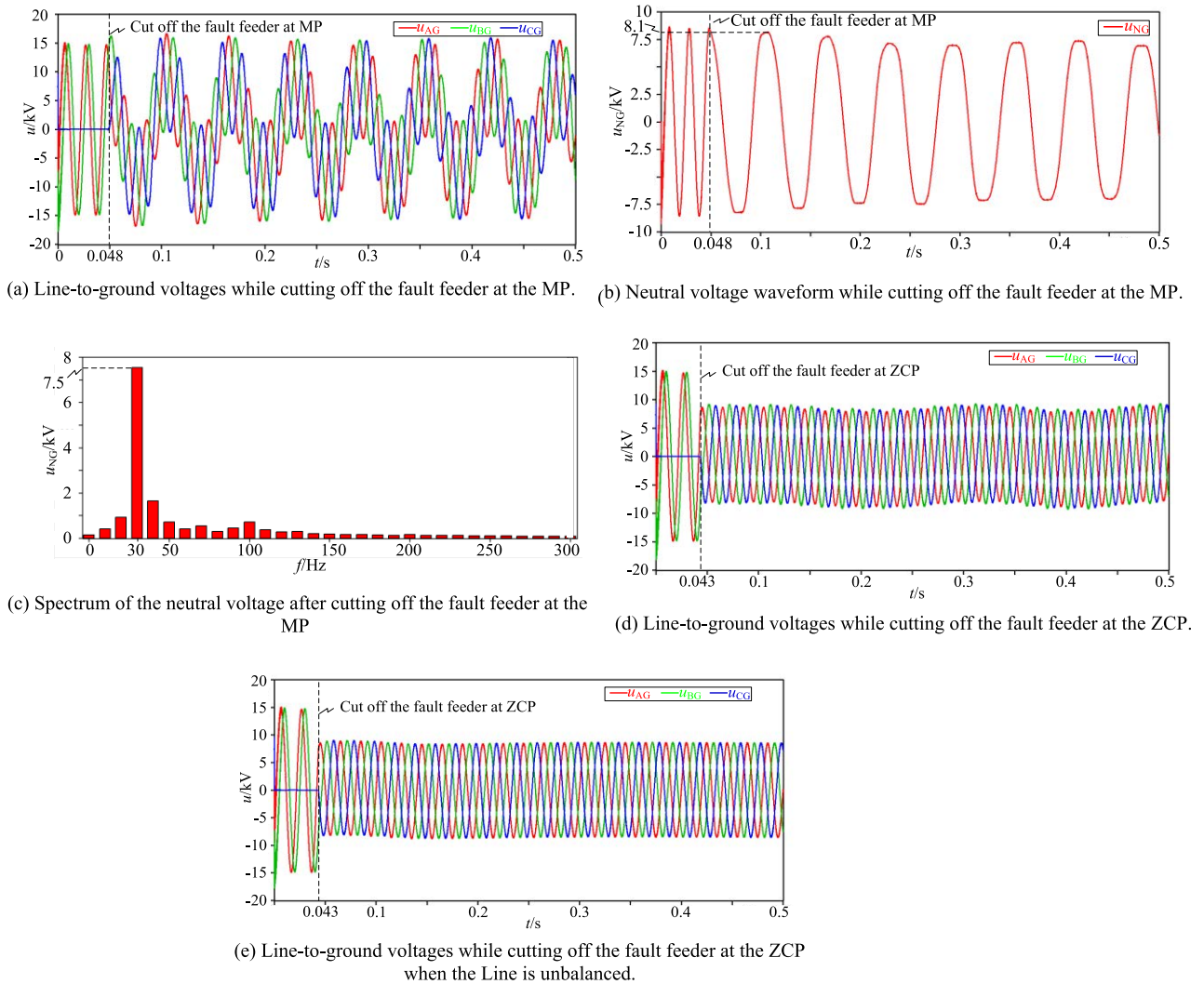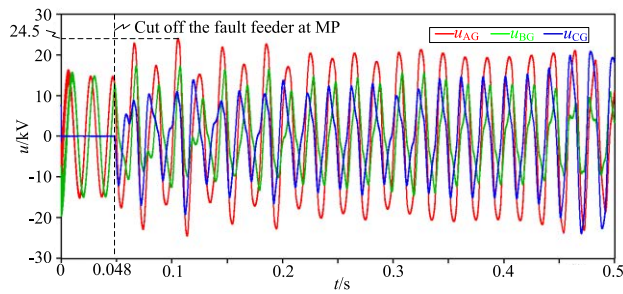
FIGURE 12. Voltage waveforms when total line length is 60 km and the fault line is cut off at the MP and ZCP.

the waveforms of the line-to-ground and neutral voltages when the fault is removed at $t = 0.048$ s (MP). It can be seen from Fig. 12a that the line-to-ground voltages fluctuate periodically, and their amplitudes all increase after the cutting-off. Obvious and continuous ferroresonance can be observed. The waveform of u_{NG} in Fig. 12b shows an 8.1 kV overvoltage and the spectrum of u_{NG} after the cutting-off shows a 7.5 kV harmonic component with the frequency of 30 Hz, which indicates that a subharmonic resonance happens. Nevertheless, the three line-to-ground voltages in Fig. 12d show that the voltages change to be balanced and in their nominal values after the cutting-off happens at the ZCP. Considering the line unbalance under the condition of frequency division resonance, the unbalance ratio is 3%, and the relative ground capacitance of phase A is 3.2 μF, that of phase B is 2.8 μF, and that of phase C is 3 μF. After modifying the relative ground capacitance, the single-phase grounding fault is removed at the ZCP, and the three-phase voltage waveform is shown in Fig. 12e. It can be seen from the figure that the removal of the fault at the ZCP

under the imbalance condition also avoids the occurrence of ferroresonance.

B. FUNDAMENTAL-FREQUENCY AND HIGH-FREQUENCY RESONANCE CONDITIONS WITHOUT SUPPRESSION MEASURES

When the excitation inductance drops greatly, the dc component in the total energy is too large due to the small excitation inductance. Cutting off the fault feeder at the ZCP, i.e., the minimum instant of the energy is not sufficient to avoid the resonance. Assume that the total length of the feeder lines is 10 km, and the capacitance-to-ground is 0.5 μF. From the line-to-ground voltages and neutral voltage waveforms in Fig. 13a and Fig. 13b, it can be observed that a 24.5 kV overvoltage (close to 3 p.u.) in line-to-ground voltages and 15 kV overvoltage (close to 1.9 p.u.) in neutral voltage occur after the fault line is cut off at the MP. The neutral voltage spectrum shows a 14.8 kV harmonic component at the fundamental frequency, which indicates the fundamental resonance.

(a) Line-to-ground voltages while cutting off the fault feeder at the MP.
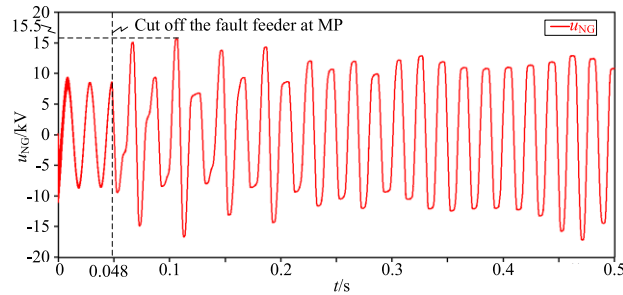
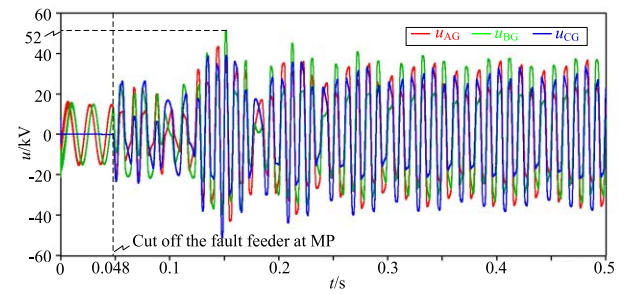(b) Neutral voltage waveform while cutting off the fault feeder at the MP.
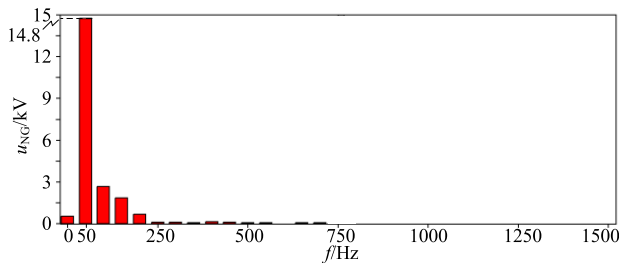
(c) Spectrum of the neutral voltage after cutting off the fault feeder at the MP.

FIGURE 13. Voltage waveforms when total line length is 10 km and the fault line is cut off at the MP and ZCP without ferroresonance suppression measure.

(a) Line-to-ground voltages while cutting off the fault feeder at the MP.

(b) Neutral voltage waveform while cutting off the fault feeder at the MP.

(c) Spectrum of the neutral voltage after cutting off the fault feeder at the MP.

FIGURE 14. Voltage waveforms when total line length is 3 km and the fault line is cut off at the MP and ZCP without ferroresonance suppression measure.
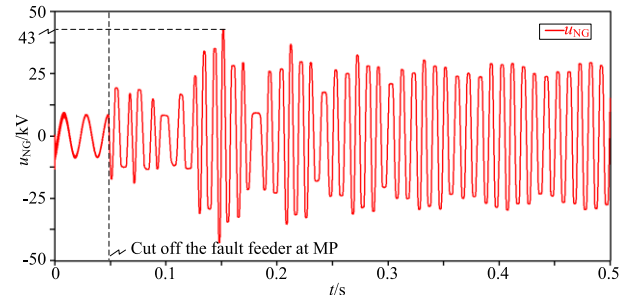
Assume that the total length of the feeder lines is 3 km, and the capacitance-to-ground is 0.15 μF. Fig. 14 shows the waveforms when the SLG fault is cut off at the MP. Overvoltage of more than 6 p.u. in the line-to-ground voltages and 5 p.u. in the neutral voltage can be observed from Fig. 14a and Fig. 14b. The spectrum of the neutral voltage after the fault feeder is cut off shows a 32.5 kV at 100 Hz, which clearly indicate a high-frequency resonance.

C. FUNDAMENTAL-FREQUENCY AND HIGH-FREQUENCY RESONANCE CONDITIONS WITH SUPPRESSION MEASURES
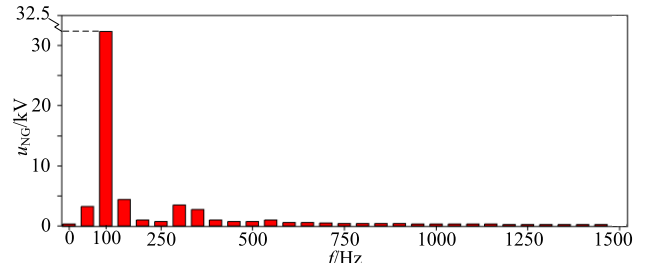
From the above simulation and analysis, it can be seen that high overvoltage occurs when the fault feeder line is cut off at the MP without ferroresonance suppression measures. The proposed method can co-ordinate with the measure and help to achieve fast ferroresonance suppression. In the following analysis, a 20 kΩ ferroresonance suppression resistance (FSR) is added between the primary-side neutral point of the PT and the ground.

The simulation waveforms under fundamental-frequency ferroresonance condition are shown in Fig. 15. The SLG fault on phase C is set at the beginning of simulation. The fault is firstly removed at the MP or the ZCP, both without ferroresonance suppression resistor. It can be seen from Fig. 15 that fundamental-frequency ferroresonance happens whenever the fault feeder is cut off. The fault is set on phase C again at $t = 0.24$ s and meanwhile the suppression resistor is connected. Then, the fault is removed at the MP and ZCP again. It can be seen clearly that if the fault is removed at the MP, transient overvoltage still exists which is higher than the magnitude of nominal phase voltage. The transient process is relatively long and lasts for more than two power supply periods. However, if the fault is removed at the ZCP, the voltage of each phase immediately reaches steady state without overvoltage and visible transient process.
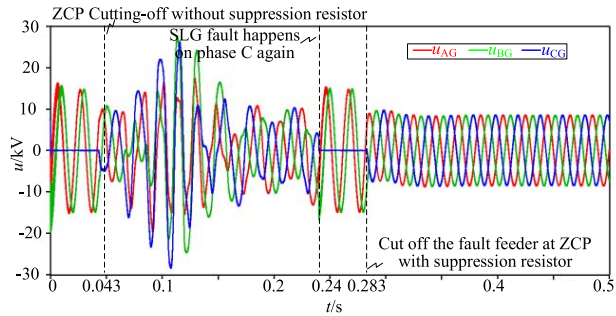
The same simulation was conducted for the high-frequency ferroresonance condition, as shown in Fig. 16.

Without the ferroresonance suppression resistor, the resonance happens whenever the fault is removed at the MP or
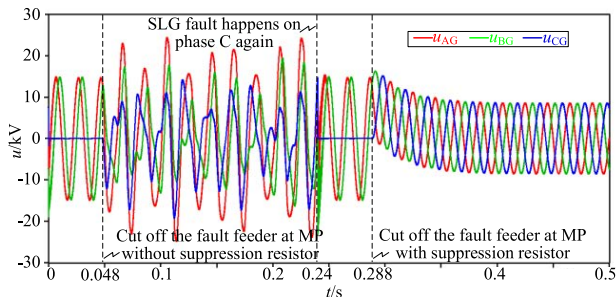
(a) Line-to-ground voltages while cutting off the fault feeder at the MP.

(b) Line-to-ground voltages while cutting off the fault feeder at the ZCP.

FIGURE 15. Comparison of the line-to-ground voltages while cutting off the fault line at the MP and ZCP with suppression resistor under fundamental-frequency resonance condition.
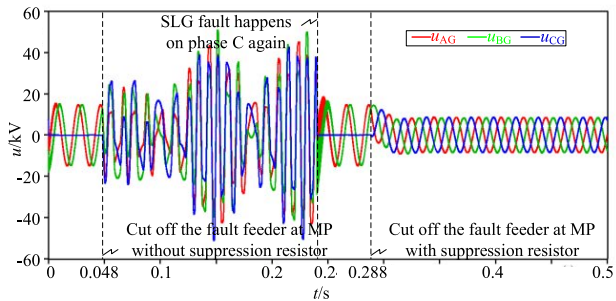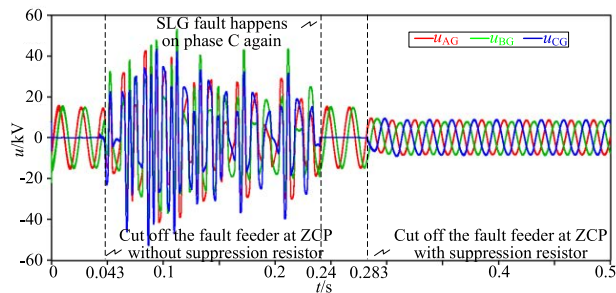

(a) Line-to-ground voltages while cutting off the fault feeder at the MP.

(b) Line-to-ground voltages while cutting off the fault feeder at the ZCP.

FIGURE 16. Comparison of the line-to-ground voltages while cutting off the fault line at the MP and ZCP with suppression resistor under high-frequency resonance condition.

the ZCP. Over 50 kV overvoltage can be observed during the resonance in both conditions. With the suppression resistor, both the two fault removal points are effective for ferroresonance avoidance. However, the transient process of the line-to-ground voltages for the MP are relatively longer

TABLE 3. Comparative simulation results.

Phase Cap. (μF)	Resonan-ce frequen-cy (Hz)	Peak neutral voltage at MP removal without FSR (p.u.)	Peak neutral voltage at ZCP removal without FSR (p.u.)	Peak neutral voltage at MP removal with FSR (p.u.)	Peak neutral voltage at ZCP removal with FSR (p.u.)
3	30	1	0.1	1.03	0.01
0.5	50	1.9	-	1.05	0.18
0.15	100	5	-	1.13	0.25

TABLE 4. PT excitation characteristic.

Secondary applied voltage(V)	11.5	28.9	46.2	57.7	69.3	109.7
Excitation current(A)	0.02	0.04	0.06	0.07	0.08	0.12

than that for the ZCP. As the latter shows almost no transient process and no overvoltage in the three-phase voltages, which is better for the safety of the power supply apparatus.

The comparative and conclusive simulation results are shown in Tab. 3. It can be observed that the proposed method has better neutral voltage avoidance performance in the subharmonic ferroresonance condition than the MP removal one. With the FSR, the proposed method reaches better neutral voltage suppression performance than its counterpart. The simulation results are consistent with the theoretical analysis.

VI. EXPERIMENTAL VERIFICATION

In order to verify the ferromagnetic resonance suppression effect of SLG fault removal at the ZCP of the neutral voltage described in this paper, a 10 kV distribution network experimental is carried out in the laboratory. The line voltage of the three-phase power supply in the experiment is 10 kV and the power frequency is 50 Hz. The line-to-ground capacitance is emulated with a 0.65 μF lumped capacitor on each phase. The model of electromagnetic voltage transformer is JDZX10-10A, and its excitation characteristics are shown in Tab. 4.

The main wiring diagram of the experimental system is shown in Fig. 17. In this experiment, the SLG fault is removed at different times to verify the ferroresonance suppression effect. The excitation condition of ferromagnetic resonance is the SLG fault removal. The experiment is divided into two parts. The first part verifies the effect of SLG fault removal on ferromagnetic resonance at the non-ZCP of the neutral voltage. The second part verifies the suppression effect of removing SLG fault when the neutral voltage is cut off at ZCP. In the experiment, k1 is closed first. After the normal operation of the distribution network,
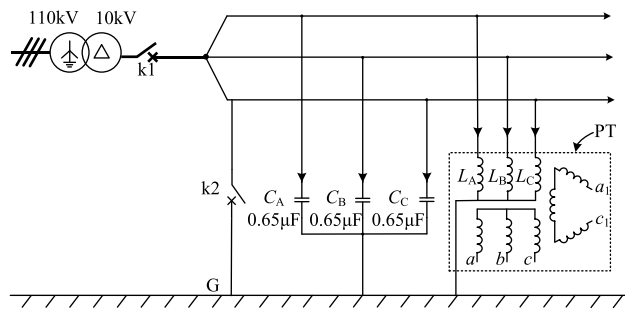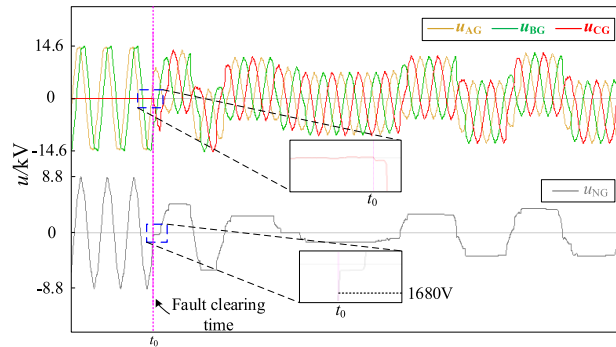
FIGURE 17. Topology of the experimental system.

FIGURE 18. Waveform diagram of the experiment of removing SLG fault at non-ZCP.
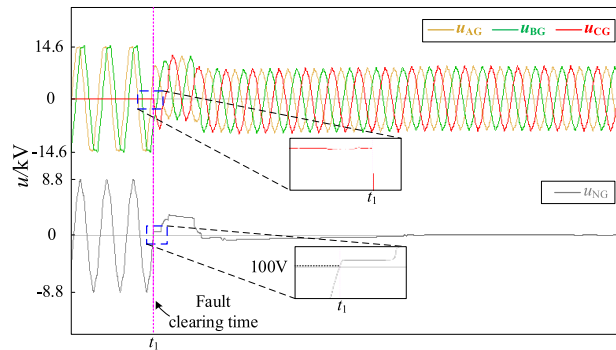

FIGURE 19. Waveform diagram of the experiment of removing SLG fault at ZCP.

the switch k2 is closed to form a C-phase metallic ground fault. A delay relay is used to disconnect k2 after certain time. From the waveforms of the phase-to-ground voltages and neutral voltage in the experiment, the influence of the SLG fault removal time on the ferromagnetic resonance can be observed. The experimental waveforms are shown in Fig. 18 and Fig. 19.

Fig. 18 is the experimental waveforms of the SLG fault removal at the non-ZCP of the neutral voltage. It can be seen that the instantaneous value of the neutral voltage at the time of removal of the SLG fault (t_0) is 1680 V. After the SLG fault is removed, a continuous subharmonic ferroresonance is excited. Fig. 19 is the experimental waveforms of the SLG fault removal at the lowest energy point, i.e., the ZCP of the neutral voltage. The instantaneous value of the neutral voltage at the moment of removal of the SLG fault (t_1) is 100 V, which is very small, thus the moment can be treated as the

zero-cross point of the neutral voltage. After the SLG fault is removed, the phase-to-ground voltages and neutral voltage are stabilized in a short time, and the ferromagnetic resonance is not excited. It can be seen that the removal of the SLG fault at the ZCP of the neutral voltage proposed in this paper can effectively avoid the occurrence of the ferromagnetic resonance.

VII. CONCLUSION

This paper has analyzed the influence of removal time of permanent SLG fault on ferroresonance in a neutral ungrounded distribution network and proposed a processing method of permanent SLG fault for ferroresonance avoidance. The contribution of this paper can be concluded as follows.

1) The zero-cross point corresponds to the minimum of the system energy, which closely relates to the occurrence and level of the ferroresonance.
2) The proposed method is effective for avoiding subharmonic resonance. When working with the ferroresonance suppression resistor, it is effective for suppressing the fundamental-frequency and high-frequency ferroresonance.

The proposed method can be implemented by the voltage-source converter based active arc suppression device which has fast response for the current instruction tracking. Further work focuses on the ferroresonance avoidance method for distribution networks with the resonance grounding method.

REFERENCES

[1] R. Martínez, M. Manana, J. I. Rodríguez, M. Álvarez, R. Mínguez, A. Arroyo, E. Bayona, F. Azcondo, A. Pigazo, and F. Cuartas, "Ferroresonance phenomena in medium-voltage isolated neutral grids: A case study," *IET Renew. Power Gener.*, vol. 13, no. 1, pp. 209–214, Jan. 2019.

[2] E. Price, "A tutorial on ferroresonance," in *Proc. 67th Annu. Conf. Protective Relay Eng.*, College Station, TX, USA, Mar. 2014, pp. 676–704.

[3] H. A. Sharbain, A. Osman, and A. El-Hag, "Detection and identification of ferroresonance," in *Proc. 7th Int. Conf. Modeling, Simulation, Appl. Optim. (ICMSAO)*, Sharjah, United Arab Emirates, Apr. 2017, pp. 1–4.

[4] T. A. Mellik, F. D. Painter, D. D. Shipp, and T. J. Dionise, "Proactive study and novel mitigation of MV power system damage due to sub-power-frequency ferro-resonance for a gas plant," *IEEE Trans. Ind. Appl.*, vol. 54, no. 4, pp. 3991–4000, Jul. 2018.

[5] D. C. McDermit, D. D. Shipp, T. J. Dionise, and V. Lorch, "Medium-voltage switching transient-induced potential transformer failures: Prediction, measurement, and practical solutions," *IEEE Trans. Ind. Appl.*, vol. 49, no. 4, pp. 1726–1737, Jul./Aug. 2013.

[6] W. Piasecki, M. Florkowski, M. Fulczyk, P. Mahonen, and W. Nowak, "Mitigating ferroresonance in voltage transformers in ungrounded MV networks," *IEEE Trans. Power Del.*, vol. 22, no. 4, pp. 2362–2369, Oct. 2007.

[7] Y. N. Ryzhkova and L. V. V. Aaron, "Transient peculiarities in resonant grounded networks," *Vestnik MEI*, vol. 15, no. 3, pp. 42–47, 2015.

[8] T. A. Mellik, T. J. Dionise, and R. Yanniello, "A case study of voltage transformer failures: Solution implementation in a modern data center," *IEEE Ind. Appl. Mag.*, vol. 24, no. 1, pp. 98–109, Jan./Feb. 2018.

[9] Y. Wang, X. Liang, I. R. Pordanjani, R. Cui, A. Jafari, and C. Clark, "Investigation of ferroresonance causing sustained high voltage at a de-energized 138 kV bus: A case study," *IEEE Trans. Ind. Appl.*, vol. 55, no. 6, pp. 5675–5686, Nov. 2019.

[10] I. R. Pordanjani, X. Liang, Y. Wang, and A. Schneider, "Single-phase ferroresonance in an ungrounded system during system energization," *IEEE Trans. Ind. Appl.*, vol. 57, no. 4, pp. 3530–3537, Jul./Aug. 2021.

[11] H. Radmanesh, "Distribution network protection using smart dual functional series resonance-based fault current and ferroresonance overvoltage limiter," *IEEE Trans. Smart Grid*, vol. 9, no. 4, pp. 3070–3078, Jul. 2018.

[12] M. Tajdinian, M. Allahbakhshi, S. Biswal, O. P. Malik, and D. Behi, "Study of the impact of switching transient overvoltages on ferroresonance of CCVT in series and shunt compensated power systems," *IEEE Trans. Ind. Informat.*, vol. 16, no. 8, pp. 5032–5041, Aug. 2020.

[13] W. Chunbao, T. Lijun, and Q. Yinglin, "A study on factors influencing ferroresonance in distribution system," in *Proc. 4th Int. Conf. Electr. Utility Deregulation Restructuring Power Technol. (DRPT)*, Weihai, China, Jul. 2011, pp. 583–588.

[14] E. Fuchs and M. A. S. Masoum, *Power Quality in Power Systems and Electrical Machines*, vol. 8. Amsterdam, The Netherlands: Elsevier, 2015, p. 1140.

[15] T.-S. Kong, H.-D. Kim, H.-S. Park, S.-H. Lee, S.-Y. Kim, P.-B. Joung, and J.-Y. Park, "Study on reliability improvement of voltage transformers by increasing voltage factor," *J. Electr. Eng. Technol.*, vol. 15, no. 3, pp. 1463–1469, May 2020.

[16] K.-H. Tseng and P.-Y. Cheng, "Mitigating 161 kV electromagnetic potential transformers' ferroresonance with damping reactors in a gas-insulated switchgear," *IET Gener. Transmiss. Distrib.*, vol. 5, no. 4, pp. 479–488, Apr. 2011.

[17] A. Heidary, K. Rouzbehi, H. Radmanesh, and J. Pou, "Voltage transformer ferroresonance: An inhibitor device," *IEEE Trans. Power Del.*, vol. 35, no. 6, pp. 2731–2733, Dec. 2020.

[18] X. Chen, "Discussion of 'modeling and analysis guidelines for slow transients—Part 3: The study of ferroresonance,'" *IEEE Trans. Power Del.*, vol. 18, no. 3, p. 1098, Jul. 2003.

[19] P. Wang, B. Chen, C. Tian, B. Sun, M. Zhou, and J. Yuan, "A novel neutral electromagnetic hybrid flexible grounding method in distribution networks," *IEEE Trans. Power Del.*, vol. 32, no. 3, pp. 1350–1358, Jun. 2017.

[20] B. Fan, G. Yao, W. Wang, X. Yang, H. Ma, K. Yu, C. Zhuo, and X. Zeng, "Faulty phase recognition method based on phase-to-ground voltages variation for neutral ungrounded distribution networks," *Electr. Power Syst. Res.*, vol. 190, Jan. 2021, Art. no. 106848.

[21] X. Yao, C. Guan, C. Wang, J. Wang, S. Ai, Z. Liu, and Y. Geng, "Design and verification of an ultra-high voltage multiple-break fast vacuum circuit breaker," *IEEE Trans. Power Del.*, early access, Nov. 18, 2021, doi: 10.1109/TPWRD.2021.3129002.

[22] W. Wang, X. Zeng, L. Yan, X. Xu, and J. M. Guerrero, "Principle and control design of active ground-fault arc suppression device for full compensation of ground current," *IEEE Trans. Ind. Electron.*, vol. 64, no. 6, pp. 4561–4570, Jun. 2017.

QIAN YU received the Ph.D. degree in business administration from the Changsha University of Science and Technology, Changsha, China, in 2021.

Since 2021, she has been an Assistant Professor with the College of Business Administration, Hunan University of Finance and Economics. Her research interests include renewable energy permeation and power systems optimization.

BISHUANG FAN (Member, IEEE) received the Ph.D. degree in control science and engineering from Zhongnan University, Changsha, China, in 2014.

He was promoted to an Associate Professor, in 2014. In 2016, he was a Visiting Scholar with The University of Tennessee, Knoxville. His current research interests include power quality and active arc suppression in distribution networks.

PENGFEI LIU received the M.S. degree in electrical engineering from the Changsha University of Science and Technology, China, in 2021.

He is currently an Engineer with State Grid Yongzhou Electric Power Company. His research interest includes the suppression analysis of ferromagnetic resonance in distribution networks.

PAN LU received the B.S. degree in electrical engineering from the Changsha University of Science and Technology, Changsha, China, in 2020, where she is currently pursuing the master's degree in electrical engineering.

Her research interests include ferromagnetic resonance suppression and flexible grounding in distribution networks.

WEN WANG (Member, IEEE) received the B.S. and Ph.D. degrees in electrical engineering from Hunan University, Changsha, China, in 2008 and 2013, respectively.

Since 2013, he has been an Assistant Professor with the School of Electrical and Information Engineering, Changsha University of Science and Technology, Changsha, where he has been promoted to an Associate Professor, since 2017. Since 2016, he has also been a Guest Researcher with the Department of Energy Technology, Aalborg University, Aalborg, Denmark. His current research interests include power electronics and grounding methods in distribution networks.

FALIANG WANG received the M.S. degree in electrical engineering from the Changsha University of Science and Technology, China, in 2019.

He is currently an Engineer with State Grid Yichun Electric Power Company. His research interest includes the suppression analysis of ferromagnetic resonance in distribution networks.

XIANGJUN ZENG (Senior Member, IEEE) received the B.S. degree from Hunan University, Changsha, China, in 1993, the M.S. degree from Wuhan University, Wuhan, China, in 1996, and the Ph.D. degree from the Huazhong University of Science and Technology, Wuhan, in 2001, all in electrical engineering.

He was a Postdoctoral Fellow with Xuji Relay Company and The Hong Kong Polytechnic University; and a Visiting Professor with Nanyang Technological University, Singapore. He is currently a Professor with the School of Electrical and Information Engineering, Changsha University of Science and Technology, Changsha. His research interest includes real-time computer applications in power systems control and protection.

• • •